normal αSyn function and its misfunction in synucleinopathies. We established that the ability of the protein to inhibit PLD, promote the accumulation of lipids, influence the balance of vesicular pools, associate with membranes in a highly selective manner, induce ubiquitin accumulation, and inhibit the proteasome when misfolded are all intrinsic and biologically relevant properties of the protein that can be uncoupled from each other by the effects of αSyn mutations. Constructs expressing mutant Q103 Htt did not produce similar biological effects (supporting online material), and unbiased genetic screens confirmed that distinct pathways are involved in αSyn and Htt toxicities (*30*). Notably, membrane-bound αSyn is in dynamic equilibrium with cytoplasmic forms. Just a twofold difference in expression was sufficient to cause a catastrophic change in its behavior, inducing nucleated polymerization and recruiting protein previously associated with membranes to cytoplasmic inclusions. This nucleated polymerization process suggests a mechanism by which even small changes in the QC balance of aging neurons could produce a toxic gain of αSyn function concomitantly with a loss of normal function. Thus, two hypotheses [gain of toxic function or loss of normal function (*31*)] put forward to explain PD can be reconciled by a single molecular mechanism.

Note added in proof: Very recently Singleton *et al*. (*32*) reported that a triplication of the αSyn locus on one chromosome (presumably doubling the expression of wild-type αSyn) causes premature onset of PD, strongly supporting our model that a small change in the expression of αSyn relative to the cell's quality-control systems causes disease-related toxicity.

References and Notes

1. C. B. Lucking, A. Brice, *Cell. Mol. Life Sci.* **57**, 1894 (2000).
2. T. Gasser, *J. Neurol.* **248**, 833 (2001).
3. T. Kitada *et al.*, *Nature* **392**, 605 (1998).
4. E. Leroy *et al.*, *Nature* **395**, 451 (1998).
5. Y. Liu, L. Fallon, H. A. Lashuel, Z. Liu, P. T. Lansbury Jr., *Cell* **111**, 209 (2002).
6. P. J. Muchowski, *Neuron* **35**, 9 (2002).
7. Materials and methods, additional data, and other supporting materials concerning data not shown are available on *Science* Online.
8. P. J. McLean, H. Kawamata, B. T. Hyman, *Neuroscience* **104**, 901 (2001).
9. T. F. Outeiro, S. Lindquist, data not shown.
10. E. Jo, J. McLaurin, C. M. Yip, P. St George-Hyslop, P. E. Fraser, *J. Biol. Chem.* **275**, 34328 (2000).
11. M. H. Polymeropoulos *et al.*, *Science* **276**, 2045 (1997).
12. R. Kruger *et al.*, *Nature Genet.* **18**, 106 (1998).
13. E. Jo, N. Fuller, R. P. Rand, P. St George-Hyslop, P. E. Fraser, *J. Mol. Biol.* **315**, 799 (2002).
14. R. Bussell Jr., D. Eliezer, *J. Mol. Biol.* **329**, 763 (2003).
15. S. J. Berke, H. L. Paulson, *Curr. Opin. Genet. Dev.* **13**, 253 (2003).
16. J. P. Taylor, J. Hardy, K. H. Fischbeck, *Science* **296**, 1991 (2002).
17. K. A. Conway *et al.*, *Proc. Natl. Acad. Sci. U.S.A.* **97**, 571 (2000).
18. A. Hershko, A. Ciechanover, A. Varshavsky, *Nature Med.* **6**, 1073 (2000).
19. L. Stefanis, K. E. Larsen, H. J. Rideout, D. Sulzer, L. A. Greene, *J. Neurosci.* **21**, 9549 (2001).
20. D. M. Sampathu, B. I. Giasson, A. C. Pawlyk, J. Q. Trojanowski, V. M. Lee, *Am. J. Pathol.* **163**, 91 (2003).
21. N. F. Bence, R. M. Sampat, R. R. Kopito, *Science* **292**, 1552 (2001).
22. D. D. Murphy, S. M. Rueter, J. Q. Trojanowski, V. M. Lee, *J. Neurosci.* **20**, 3214 (2000).
23. N. B. Cole *et al.*, *J. Biol. Chem.* **277**, 6344 (2002).
24. J. M. Jenco, A. Rawlingson, B. Daniels, A. J. Morris, *Biochemistry* **37**, 4901 (1998).
25. V. A. Bankaitis, J. R. Aitken, A. E. Cleves, W. Dowhan, *Nature* **347**, 561 (1990).
26. S. A. Rudge, T. R. Pettitt, C. Zhou, M. J. Wakelam, J. A. Engebrecht, *Genetics* **158**, 1431 (2001).
27. A. Sreenivas, J. L. Patton-Vogt, V. Bruno, P. Griac, S. A. Henry, *J. Biol. Chem.* **273**, 16635 (1998).
28. R. Sharon *et al.*, *Proc. Natl. Acad. Sci. U.S.A.* **98**, 9110 (2001).
29. R. Sharon *et al.*, *Neuron* **37**, 583 (2003).
30. S. Willingham, T. F. Outeiro, M. J. DeVit, S. L. Lindquist, P. J. Muchowski, *Science* **302**, 1769 (2003).
31. T. M. Dawson, V. L. Dawson, *J. Clin. Invest.* **111**, 145 (2003).
32. A.B. Singleton *et al.*, *Science* **302**, 841 (2003).

33. This work was funded by NIH/National Institute of Neurological Disorders and Stroke (grant NS044829-01). T.F.O. was partially supported by Programa Praxis XXI, Fundacao para a Ciencia e Tecnologia, Portugal. We thank P. Lansbury, R. Esposito, J. Engebrecht, H. Chang, and S. Henry for plasmids and strains and members of the Lindquist laboratory for critical reading of this manuscript.

Supporting Online Material

www.sciencemag.org/cgi/content/full/302/5651/1772/DC1
Materials and Methods
Figs. S1 to S4
Tables S1 and S2
References

14 August 2003; accepted 13 October 2003

Regulation of Cell Polarity and Protrusion Formation by Targeting RhoA for Degradation

Hong-Rui Wang,*[1] Yue Zhang,*[1] Barish Ozdamar,[1,2] Abiodun A. Ogunjimi,[1] Evguenia Alexandrova,[3] Gerald H. Thomsen,[3] Jeffrey L. Wrana[1,2]†

The Rho family of small guanosine triphosphatases regulates actin cytoskeleton dynamics that underlie cellular functions such as cell shape changes, migration, and polarity. We found that Smurf1, a HECT domain E3 ubiquitin ligase, regulated cell polarity and protrusive activity and was required to maintain the transformed morphology and motility of a tumor cell. Atypical protein kinase C zeta (PKCζ), an effector of the Cdc42/Rac1-PAR6 polarity complex, recruited Smurf1 to cellular protrusions, where it controlled the local level of RhoA. Smurf1 thus links the polarity complex to degradation of RhoA in lamellipodia and filopodia to prevent RhoA signaling during dynamic membrane movements.

The Rho family of small guanosine triphosphatases (GTPases) cycle between an active guanosine 5′-triphosphate (GTP)–bound and inactive guanosine 5′-diphosphate (GDP)–bound state to control cell shape, motility, polarity, and behavior (*1*–*5*). At the leading edge of motile cells, Cdc42 and Rac1 regulate the actin cytoskeleton to form fingerlike filopodia and sheetlike lamellipodia, respectively, whereas in the cell body RhoA induces assembly of focal adhesions and contractile actin-myosin stress fibers. Active Rho GTPases signal through effector complexes (*5*, *6*), one of which is the PAR (for partitioning defective) polarity complex (*7*). PAR6 is a key component of this complex that binds atypical protein kinase C zeta (PKCζ) (*8*–*10*), recruits it to active Cdc42 (*8*–*10*), and is important for cell transformation (*10*), polarity (*11*, *12*), and epithelial tight junctions (*9*, *13*–*15*). One effector pathway of this complex involves GSK-3β and APC, which links PAR6 to microtubules and astrocyte polarity (*16*); another, involving Lgl, affects asymmetric cell divisions (*17*) and polarization of migrating cells (*18*). A direct link between the polarity complex and regulation of actin cytoskeleton dynamics has not been defined.

Conjugation of polyubiquitin chains to protein targets triggers their degradation and is mediated by E3 enzymes, which include the Smurf family of C2-WW-HECT ubiquitin ligases (*19*, *20*) that regulate transforming growth factor–β (TGF-β) signal transduction (*21*–*23*). Ubiquitin ligases are not known to regulate cell shape, motility, and polarity.

[1]Program in Molecular Biology and Cancer, Samuel Lunenfeld Research Institute, Mount Sinai Hospital, Toronto M56 1×5, Canada. [2]Department of Medical Genetics and Microbiology, University of Toronto, Toronto M5S 1A8, Canada. [3]Department of Biochemistry and Cell Biology, Center for Developmental Genetics, CMM 348, Stony Brook University, Stony Brook, NY 11794–5215, USA.

*These authors contributed equally to this work.
†To whom correspondence should be addressed. E-mail: wrana@mshri.on.ca

However, when Smurf1 or yellow fluorescent protein (YFP)–tagged Smurf1 was overexpressed in Mv1Lu epithelial cells, we observed large numbers of dynamic protrusions in 95% of expressing cells (*24*). These were not present in the controls, nor in cells expressing a catalytic mutant of Smurf1, YFP-Smurf1(C699A) (Movies S1 and S2) (Fig. 1A). Furthermore, movement of YFP-Smurf1 to the tips of processes often preceded active extension (Fig. 1A), whereas movement to the cell body presaged retraction (Movie S1). Smurf1 expression also strongly reduced stress fiber formation (Movie S1). In contrast, Smurf2 rarely induced protrusive activity (15% of Smurf2-expressing cells). Next, we examined how increased expression of Smurf1 affected the behavior of NIH3T3 fibroblasts in a wounding assay in which cells are induced to polarize and migrate into a wound that is created by scratching the monolayer with a pipette tip. In controls, the leading-edge cells displayed organized migration (fig. S1), whereas Smurf1-expressing cells were highly disorganized and extended more protrusions at the leading edge (2.4 protrusions per cell in Smurf1-expressing populations versus 1.3 in the controls) (Fig. 1B). This suggested that Smurf1 disrupted polarity, which we examined directly by analyzing the localization of pericentrin, a component of the microtubule organization center (MTOC) (*25*) (fig. S1). In controls, 76 ± 8% of cells at the wound edge exhibited polarized MTOC localization, compared with 30 ± 6% in wild-type Smurf1-expressing cells, indicating nearly random (25%) polarity (Fig. 1B). In contrast, Smurf1(C699A) had only slight effects on protrusive activity and MTOC polarity. Thus, elevated Smurf1 expression induces protrusive activity and disrupts fibroblast polarity in a manner that is dependent on the catalytic activity of its HECT domain.

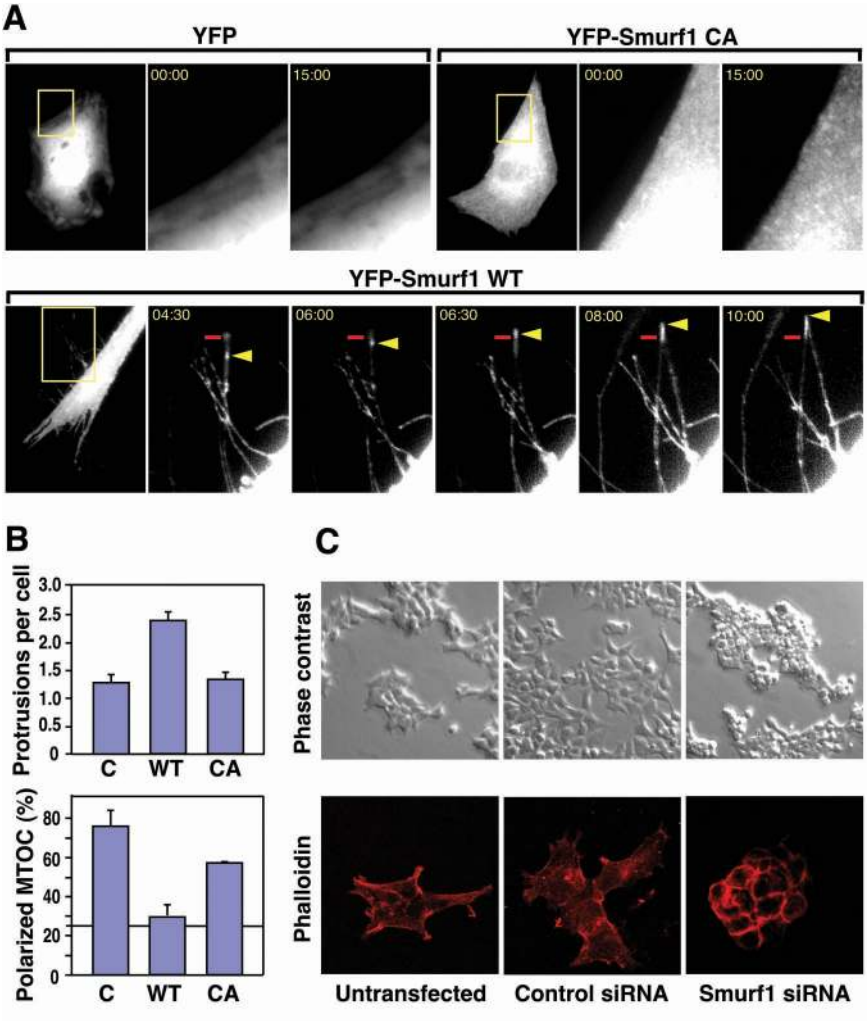

Fig. 1. Smurf1 is localized to lamellipodia and filopodia and regulates protrusive activity, polarity, and motility. (**A**) Mv1Lu cells were transfected with YFP control or YFP fused to wild-type Smurf1 (WT) or Smurf1(C699A) (CA) and imaged by time lapse fluorescence microscopy. Shown are frames extracted from the supplemental movies at the indicated times (in minutes). The start position of the tip of a protrusion in a YFP-Smurf1–expressing cell at the beginning of data collection (time 0) is marked (red bar), and movement of the YFP-Smurf1 puncta is shown highlighted (yellow arrowhead). Note that extension of the tip coincides with the arrival of Smurf1 at the tip. (**B**) Regulation of protrusive activity and polarity in NIH3T3 cells. (Top) Protrusions formed per cell in a NIH3T3 wounding assay were quantitated (mean ± SEM) and are plotted for each of the indicated cell lines. (Bottom) Polarity was measured by counting the percentage (±SEM) of cells in the front row that oriented their MTOC in the forward-facing quadrant. (**C**) Loss of protrusions and actin cytoskeleton rearrangements induced by Smurf1 siRNA. HEK293T cells were transfected with control or Smurf1 siRNA and visualized 40 hours later by phase contrast microscopy (top) or Texas red–phalloidin staining (red; bottom).

To determine the importance of endogenous Smurf1 on protrusive activity, we designed small interfering RNA (siRNA) to Smurf1 that reduced Smurf1 protein by 60% compared with controls (fig. S2A). We used the human embryonic kidney (HEK) 293T tumor cell line because these cells are highly transfectable, express Smurf1, extend many cellular protrusions, and display a disorganized actin cytoskeleton typical of a transformed phenotype (Fig. 1C). Examination of the morphology of Smurf1 siRNA-transfected cells revealed a marked change at 40 hours after transfection. The cells lost their protrusions, the actin cytoskeleton was rearranged into a cortical F-actin staining pattern, and the cells assumed a cuboidal morphology (Fig. 1C). Similar effects were observed with a second siRNA directed to Smurf1. In addition, HEK293T motility through modified Boyden chambers was reduced sixfold (fig. S3). These data indicate that Smurf1 plays an important role in regulating protrusive activity and the transformed phenotype of HEK293T cells.

Elevated expression of the Rho family GTPases Cdc42 or Rac1 induces high levels of protrusive activity, disrupts polarity, and contributes to cell transformation (*26*, *27*). Previous studies have established that the PAR6-PKCζ complex is a key effector of Cdc42 and Rac1 that controls polarity, is localized at lamellipodia and filopodia, and is required for the oncogenic activities of Cdc42 and Rac1 (*8*–*11*). PKCζ activity also mediates the loss of stress fibers caused by activated Cdc42 (*26*), and in HEK293T cells PKCζ inhibitors caused morphological changes that were similar to those in Smurf1 siRNA-treated cells (*28*). All of this suggested that Smurf1 might function as an effector of this complex. In support of this notion, in Mv1Lu and NIH3T3 cells, Smurf1 was localized to both lamellipodial- and filopodial-like protrusions (Fig. 2, A and B), where it colocalized extensively with PKCζ (Fig. 2B). Furthermore, both the expression of Smurf1 and the kinase activity of PKCζ were required for the localization of both proteins to

membrane protrusions (fig. S4, A and B). This is consistent with the requirement for atypical PKC activity in the assembly and function of PAR complexes in *Caenorhabditis elegans* and during tight junction formation in epithelial cells (*13*, *14*, *29*, *30*). Next, we demonstrated that endogenous PKCζ bound Smurf1 and that this was unaffected by treatment with PKCζ kinase inhibitors (Fig. 2C). Similar kinase-independent interactions were observed between bacterially produced proteins (fig. S4C) and in transiently transfected HEK293T cells, where the steady-state level of PKCζ was unaffected by Smurf1 (fig. S4D). This indicates that PKCζ is not a substrate of Smurf1. Thus, PKCζ binds directly to Smurf1 independent of its kinase activity, but both the expression of Smurf1 and PKCζ kinase activity are required to localize the complex to filopodia and lamellipodia.

We hypothesized that Smurf1 might be an effector of the Cdc42-PAR6-PKCζ polarity complex that mediates the ubiquitin-dependent degradation of RhoA. In support of this, wild-type Smurf1, but neither Smurf2 nor catalytically inactive Smurf1, decreased the steady-state level of RhoA, but had no effect on Cdc42 or Rac1 (Fig. 3A); this result was confirmed with the UPR assay (*31*) (fig. S5). Two proteasome inhibitors, LLnL and lactacystin, reversed this effect (Fig. 3B) (*28*). Furthermore, Smurf1 expression markedly increased ubiquitin-conjugated RhoA, whereas Smurf1(C699A) blocked all detectable ubiquitination of RhoA (Fig. 3C). Next, we examined RhoA interaction with Smurf1, using catalytically inactive Smurf1 to trap the ligase substrate (*21*, *32*, *33*). Smurf1(C699A) was found to interact with the dominant inactive form of RhoA, $RhoA^{N19}$ (Fig. 3D), which binds constitutively to guanine nucleotide exchange factors (GEFs) (*34*). Smurf1 also interacted in vitro with either nucleotide-free or GDP-bound RhoA, whereas loading with GTPγS inhibited the interaction (Fig. 3E). Because most GDP-bound RhoA in cells is associated with guanine dissociation inhibitor (GDI) (*35*), these results suggest that GDI may inhibit binding of Smurf1 to GDP-bound RhoA in mammalian cells. Finally, Smurf1 directly catalyzed ubiquitination of RhoA in an in vitro ubiquitination assay (Fig. 3F). Thus, RhoA is a direct substrate of Smurf1, and degradation of RhoA in mammalian cells may require nucleotide exchange and be dependent on a Rho GEF.

The PKCζ-dependent recruitment of Smurf1 to active membrane protrusions suggested that at endogenous levels of expression, Smurf1 activity toward RhoA was restricted to sites where the Smurf1-PKCζ complex assembled with Cdc42-PAR6 to induce membrane protrusions. Consistent with this notion, we did not see marked changes in total RhoA protein levels upon reducing Smurf1 expression (*28*). Thus, we considered that the morphological change in HEK293T cells treated with Smurf1 siRNA might be due to ectopic accumulation of RhoA in protrusions. To test this hypothesis, we examined endogenous RhoA localization at 18 hours after Smurf1 siRNA treatment. At this early time point—before morphological changes have occurred—we observed strong accumulations of RhoA and colocalized F-actin in the tips of most cellular protrusions. We also observed the initiation of RhoA accumulation at cell-cell junctions (Fig. 4A). Thus, the maintenance of low local levels of RhoA in protrusions was dependent on endogenous Smurf1. To demonstrate that RhoA degradation was a key target for Smurf1-dependent regulation of the transformed phenotype of HEK293T cells, we next tested the epistatic relation between Smurf1 and RhoA using siRNA. siRNA directed to RhoA blocked expression of the protein (fig. S2B and Fig. 4B), but had no effect on the morphology (fig. S6A) or F-actin distribution in HEK293T cells (Fig. 4B). This result indicates that there was little RhoA-dependent regulation of the actin cytoskeleton in these cells, consistent with the absence of a discernible, well-organized stress fiber network. Notably, cotransfection with RhoA siRNA strongly suppressed the effect of Smurf1 siRNA (fig. S6A and Fig. 4B). Thus, reducing RhoA expression blocks the morphological transformation and actin cytoskeleton rearrangements caused by reducing Smurf1 levels. We also observed that siRNA to RhoA severely impaired MTOC polarity in NIH3T3 cells (fig. S6B), supporting the notion that Smurf1 targeting of RhoA is important for regulating polarity. Our results point to a key role for Smurf1 as an effector of PKCζ that regulates actin cytoskeleton dynamics during protrusion formation by targeting the localized degradation of RhoA via a ubiquitin-dependent mechanism.

Regulation of cell polarity and shape by RhoGTPase-dependent regulation of the actin cytoskeleton is a key biological pathway that governs diverse cell functions such as localization of embryonic determinants, establishment of tissue and organ architecture, and cell motility. The precise temporal and spatial coordination of Rho family GTPase activity is important in a broad range of cellular activities (*2*–*5*). Our findings strongly suggest that Smurf1 is a key effector of the Cdc42/Rac1-PAR6-PKCζ pathway that antagonizes RhoA through ubiquitin-dependent degradation. In cells in which Smurf1 expression is knocked down by siRNA, RhoA and associated F-actin accumulate in cellular protrusions, indicating that the activity of

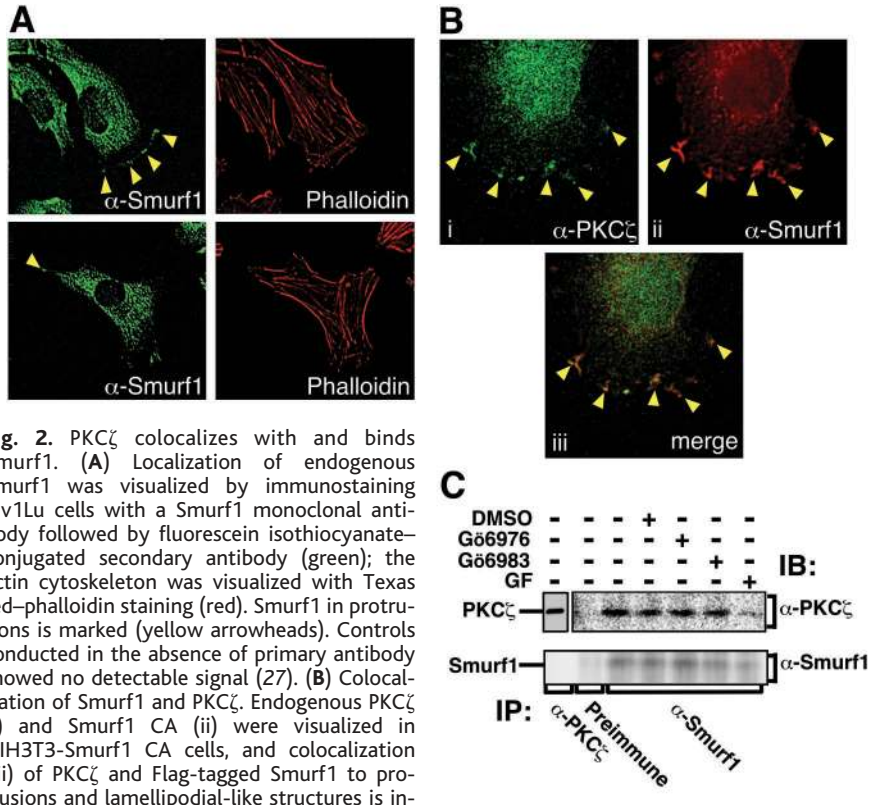

Fig. 2. PKCζ colocalizes with and binds Smurf1. (**A**) Localization of endogenous Smurf1 was visualized by immunostaining Mv1Lu cells with a Smurf1 monoclonal antibody followed by fluorescein isothiocyanate–conjugated secondary antibody (green); the actin cytoskeleton was visualized with Texas red–phalloidin staining (red). Smurf1 in protrusions is marked (yellow arrowheads). Controls conducted in the absence of primary antibody showed no detectable signal (*27*). (**B**) Colocalization of Smurf1 and PKCζ. Endogenous PKCζ (i) and Smurf1 CA (ii) were visualized in NIH3T3-Smurf1 CA cells, and colocalization (iii) of PKCζ and Flag-tagged Smurf1 to protrusions and lamellipodial-like structures is indicated (yellow arrowheads). (**C**) Interaction of endogenous Smurf1 and PKCζ in Mv1Lu cells. Lysates prepared from cells incubated in the absence or presence of the indicated inhibitors were subjected to immunoprecipitation with rabbit antibody to Smurf1 (anti-Smurf1) followed by immunoblotting with anti-PKCζ.

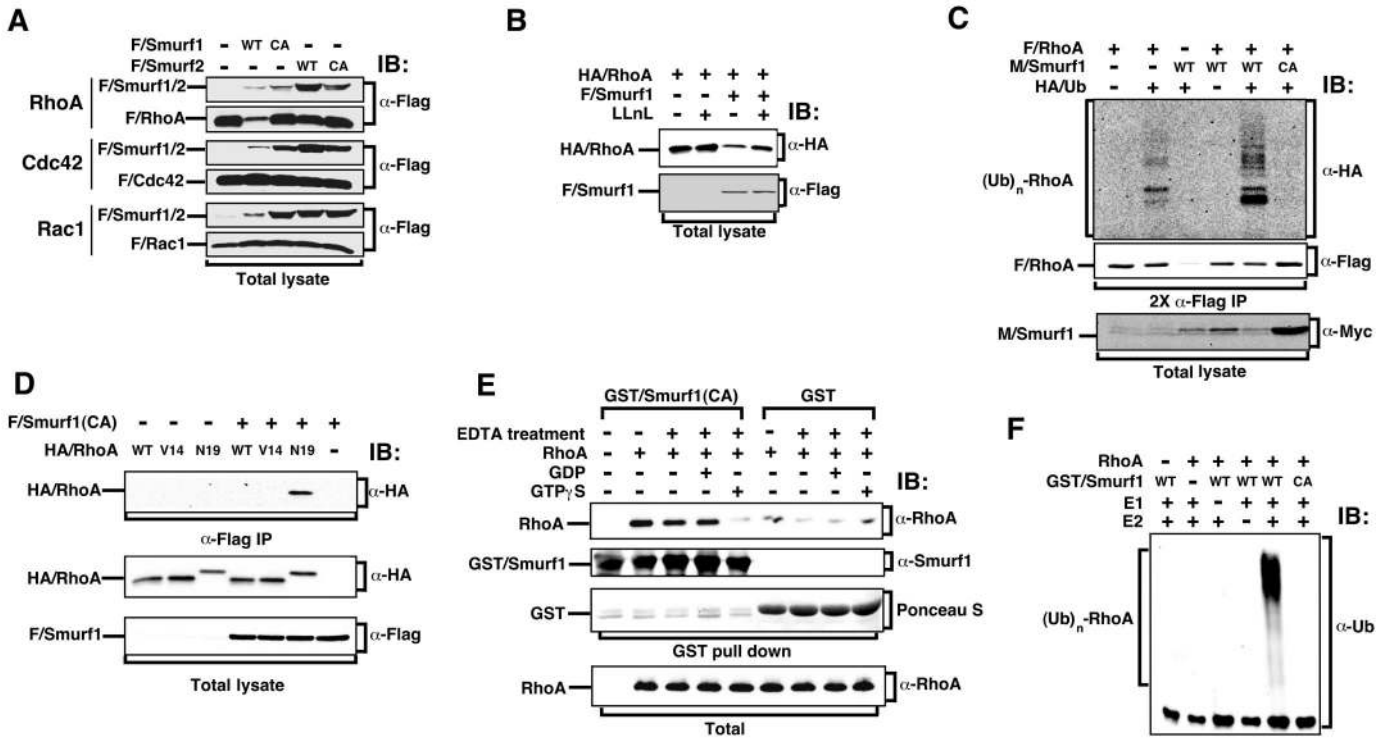

Fig. 3. Smurf1 targets RhoA for ubiquitination and degradation through ubiquitin-dependent proteasome pathway. (**A**) Expression of Smurf1 decreases the steady-state level of RhoA. HEK293T cells were transiently transfected with the indicated combinations of wild-type (WT) or catalytically inactive (CA) Flag-tagged Smurf1 (F/Smurf1) or Flag-tagged Smurf2 (F/Smurf2) and Flag-tagged RhoA (F/RhoA), Cdc42 (F/Cdc42), or Rac1 (F/Rac1). Steady-state protein levels were determined by immunoblotting (IB) total cell lysates with anti-Flag. (**B**) Proteasome inhibitors decrease RhoA down-regulation by Smurf1. HEK293T cells transfected with hemagglutinin (HA)–tagged RhoA (HA/RhoA) and F/Smurf1 were treated for 4 hours with or without 40 μM LLnL, and RhoA steady-state levels determined. (**C**) Ubiquitination of RhoA in HEK293T cells. After overnight treatment with 20 μM LLnL, lysates from cells transfected with HA-tagged ubiquitin (HA/Ub), F/RhoA, or Myc-tagged Smurf1 (M/Smurf1) (WT or CA) were subjected to anti-Flag immunoprecipitation, eluted by boiling in 1% SDS, and then reprecipitated with anti-Flag (2X IP). Ubiquitin-conjugated RhoA [$(Ub)_n$-RhoA] and free RhoA were detected by immunoblotting with the appropriate antibodies. M/Smurf1 expression was confirmed by anti-Myc immunoblotting samples of total lysates. (**D**) Interaction of Smurf1 with RhoA. HEK293T cells were transfected with F/Smurf1(CA) and various versions of HA/RhoA (WT, V14, or N19). Cell lysates were subjected to anti-Flag immunoprecipitation followed by immunoblotting (IB) with rat anti-HA to detect associated RhoA. Total protein expression was confirmed by immunoblotting as shown. (**E**) Interaction between Smurf1 and RhoA in vitro. Samples of bacterially produced RhoA treated with or without 0.25 mM GDP or GTPγS, as indicated, were incubated with glutathione beads coupled to glutathione *S*-transferase (GST) or GST/Smurf1(CA). Associated RhoA (top) and input RhoA (bottom) were determined by immunoblotting (IB) with the indicated antibody. GST was detected by Ponceau S staining. (**F**) Direct ubiquitination of RhoA by Smurf1. RhoA and WT or C699A Smurf1 were purified from bacteria and subjected to an in vitro ubiquitination assay.

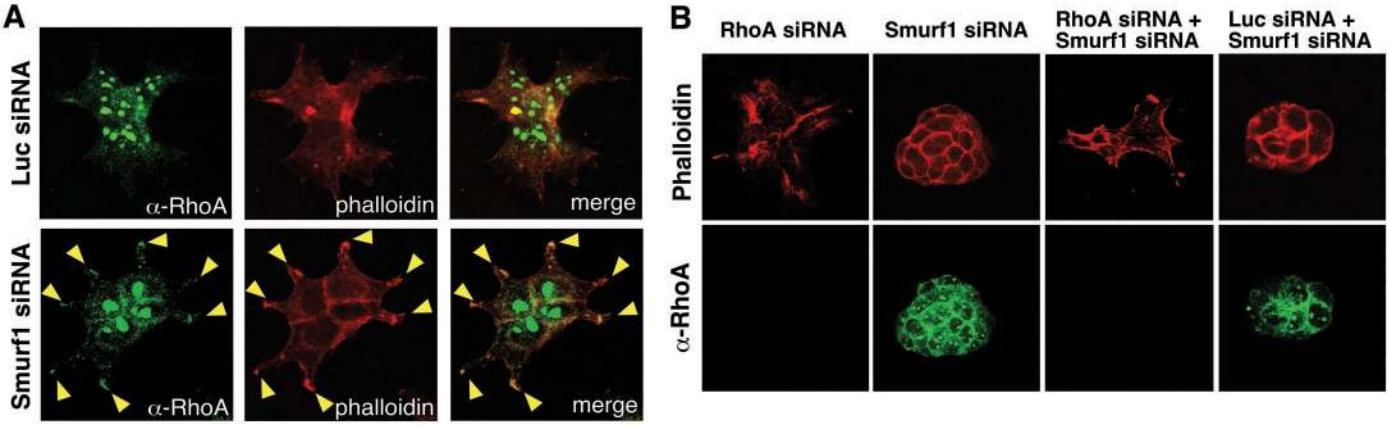

Fig. 4. Endogenous RhoA is targeted by Smurf1 in protrusions. (**A**) Reduction in Smurf1 leads to appearance of endogenous RhoA in protrusions of HEK293T cells. HEK293T cells transfected with luciferase control or Smurf1 siRNA as indicated were fixed 18 hours after transfection. Endogenous RhoA staining was visualized with an anti-RhoA primary antibody (green), and actin was detected with Texas red–conjugated phalloidin (red). Superimposition of the images (merge) reveals colocalization of RhoA and F-actin in the protrusions of Smurf1 siRNA-treated HEK293T cells (yellow arrowheads). (**B**) Reduction of endogenous RhoA by RhoA siRNA rescues the morphological change caused by Smurf1 siRNA. HEK293T cells were transfected with Smurf1, RhoA, or control siRNA, as indicated. Cells were fixed 40 hours after transfection, and RhoA and F actin were visualized by immunofluorescence microscopy as described in (A).

Smurf1 toward RhoA is locally restricted to sites of active protrusion. This is likely to be achieved through PKCζ-dependent recruitment of Smurf1 to filopodia and lamellipodia, which is in agreement with a key role for this kinase in controlling the activity of the polarity complex both in *C. elegans* (*29*, *30*) and in mammals (*13*, *14*). Furthermore, we showed that Smurf1 binds RhoA in a GEF-dependent manner, suggesting that Smurf1 activity is further restricted by a RhoA GEF that colocalizes with the polarity complex in filopodia and lamellipodia. Localizing the degradation of RhoA to protrusive regions likely acts to prevent inappropriate stress fiber formation during dynamic actin cytoskeletal remodeling that is required to drive rapid filopodial and lamellipodial membrane extensions in response to Cdc42 and Rac1 activation. Moreover, our observation that knocking down Smurf1 expression suppresses the tumorigenic morphology and motility of HEK293T cells suggests that this pathway plays a key role in maintaining the protrusive activity and transformed phenotype of cancer cells.

References and Notes

1. S. Etienne-Manneville, A. Hall, *Nature* **420**, 629 (2002).
2. D. Bar-Sagi, A. Hall, *Cell* **103**, 227 (2000).
3. A. L. Bishop, A. Hall, *Biochem. J.* **348**, 241 (2000).
4. A. Hall, C. D. Nobes, *Philos. Trans. R. Soc. London B Biol. Sci.* **355**, 965 (2000).
5. L. Van Aelst, M. Symons, *Genes Dev.* **16**, 1032 (2002).
6. A. Hall, *Br. J. Cancer* **80** (suppl. 1), 25 (1999).
7. J. E. Gomes, B. Bowerman, *Curr. Biol.* **12**, R444 (2002).
8. D. Lin *et al.*, *Nature Cell Biol.* **2**, 540 (2000).
9. G. Joberty, C. Petersen, L. Gao, I. G. Macara, *Nature Cell Biol.* **2**, 531 (2000).
10. R. G. Qiu, A. Abo, G. Steven Martin, *Curr. Biol.* **10**, 697 (2000).
11. S. Etienne-Manneville, A. Hall, *Cell* **106**, 489 (2001).
12. S.-H. Shi, L. Y. Jan, Y.-N. Jan, *Cell* **112**, 63 (2003).
13. L. Gao, G. Joberty, I. G. Macara, *Curr. Biol.* **12**, 221 (2002).
14. A. Suzuki *et al.*, *J. Cell Sci.* **115**, 3565 (2002).
15. A. Suzuki *et al.*, *J. Cell Biol.* **152**, 1183 (2001).
16. S. Etienne-Manneville, A. Hall, *Nature* **421**, 753 (2003).
17. J. Betschinger, K. Mechtler, J. A. Knoblich, *Nature* **422**, 326 (2003).
18. P. J. Plant *et al.*, *Nature Cell Biol.* **5**, 301 (2003).
19. K. F. Harvey, S. Kumar, *Trends Cell Biol.* **9**, 166 (1999).
20. A. Hershko, A. Ciechanover, *Annu. Rev. Biochem.* **67**, 425 (1998).
21. H. Zhu, P. Kavsak, S. Abdollah, J. L. Wrana, G. H. Thomsen, *Nature* **400**, 687 (1999).
22. Y. Zhang, C. Chang, D. J. Gehling, A. Hemmati-Brivanlou, R. Derynck, *Proc. Natl. Acad. Sci. U.S.A.* **98**, 974 (2001).
23. X. Lin, M. Liang, X.-H. Feng, *J. Biol. Chem.* **275**, 36818 (2000).
24. Materials and methods are available as supporting material on *Science* Online.
25. C. D. Nobes, A. Hall, *J. Cell Biol.* **144**, 1235 (1999).
26. M. P. Coghlan, M. M. Chou, C. L. Carpenter, *Mol. Cell. Biol.* **20**, 2880 (2000).
27. R. G. Qiu, A. Abo, F. McCormick, M. Symons, *Mol. Cell. Biol.* **17**, 3449 (1997).
28. H.-R. Wang, Y. Zhang, B. Ozdamar, J. L. Wrana, unpublished data.
29. T. J. Hung, K. J. Kemphues, *Development* **126**, 127 (1999).
30. Y. Tabuse *et al.*, *Development* **125**, 3607 (1998).
31. F. Levy, N. Johnsson, T. Rumenapf, A. Varshavsky, *Proc. Natl. Acad. Sci. U.S.A.* **93**, 4907 (1996).
32. P. Kavsak *et al.*, *Mol. Cell* **6**, 1365 (2000).
33. S. Bonni *et al.*, *Nature Cell Biol.* **3**, 587 (2001).
34. A. Schmidt, A. Hall, *Genes Dev.* **16**, 1587 (2002).
35. K. Kaibuchi, S. Kuroda, M. Amano, *Annu. Rev. Biochem.* **68**, 459 (1999).

36. We thank L. Attisano and members of the Wrana laboratory for discussion and comments on the manuscript; S. Elowe, D. Lin, T. Pawson, I. B. Weinstein, D. Bohmann, J. Sheng, and A. Varshavsky for providing reagents; S. Kulkarni for help with deconvolution microscopy and time-lapse imaging; and L. Locke for advice on the motility assay. We are indebted to J. Trimmer and L. Buckwalder for help in preparation of monoclonal antibodies. This work was supported by grants from the Canadian Cancer Society and the Canadian Institutes of Health Research (J.L.W.) and NIH grant HD32429 and Carol M. Baldwin Breast Cancer Foundation (G.H.T.). Y.Z. and B.O. are supported by a Canadian Institutes of Health Research (CIHR) Postdoctoral Fellowship and Doctoral Studentship awards, respectively, and E.A. is the recipient of an Institute for Cell and Developmental Biology Predoctoral Fellowship from Stony Brook University. J.L.W. is a CIHR Investigator and an International Scholar of the Howard Hughes Medical Institute.

Supporting Online Material
www.sciencemag.org/cgi/content/full/302/5651/1775/DC1
Materials and Methods
Figs. S1 to S6
Movies S1 and S2

25 August 2003; accepted 16 October 2003

Redox Regulation of Germline and Vulval Development in *Caenorhabditis elegans*

Yukimasa Shibata,* Robyn Branicky, Irene Oviedo Landaverde, Siegfried Hekimi†

In vitro studies have indicated that reactive oxygen species (ROS) and the oxidation of signaling molecules are important mediators of signal transduction. We have identified two pathways by which the altered redox chemistry of the *clk-1* mutants of *Caenorhabditis elegans* acts in vivo on germline development. One pathway depends on the oxidation of an analog of vertebrate low density lipoprotein (LDL) and acts on the germline through the Ack-related tyrosine kinase (ARK-1) kinase and inositol trisphosphate (IP_3) signaling. The other pathway is the oncogenic *ras* signaling pathway, whose action on germline as well as vulval development appears to be modulated by cytoplasmic ROS.

Reactive oxygen species (ROS) are short-lived reactive molecules that can modify cellular components including nucleic acids, proteins, and lipids. For example, the oxidation of LDLs by ROS is one of the causative factors of atherosclerosis (*1*). ROS are toxic but the oxidation of macromolecules can also serve as a signaling device (*2*). Moreover, in vitro studies have shown that ROS act as intracellular messengers in signal transduction pathways, such as *ras* signaling (*3*, *4*). However, little is known about the effect of ROS on signal transduction in intact animals (*5*).

Ubiquinone (UQ or coenzyme Q) is a redox-active lipid that has numerous biochemical roles and is involved in the production of ROS. However, UQ is also an antioxidant that prevents the initiation and/or propagation of lipid peroxidation in cellular membranes (*6*). The *Caenorhabditis elegans clk-1* gene encodes a conserved enzyme that is necessary for UQ biosynthesis (*7*). In the absence of CLK-1, mutants accumulate demethoxyubiquinone (DMQ) (*8*, *9*), which can partially replace UQ as an electron carrier (*8*). However, *clk-1* mutants require dietary UQ for their survival (*9*, *10*).

clk-1 mutants show a highly pleiotropic phenotype that includes an average slowing down and deregulation of a number of physiological processes, including aging (*11*). Presumably, given that *clk-1* mutants obtain significant amounts of UQ from their diet (*12*), these phenotypes result from the presence of DMQ, which might be a better antioxidant than UQ (*13*). Thus, the *clk-1* mutant phenotypes could be the consequence of altered redox signaling.

In addition to the previously described phenotypes, we find that somatic and germline development are desynchronized in *clk-1* mutants. In wild-type hermaphrodites, primary spermatocytes and sperm are observed at the late fourth larval stage (L4), and oogenesis commences shortly after the adult molt (Fig. 1). However, the majority of *clk-1* mutants are either before or in the process of spermatogenesis at the adult molt (fig. S1A), and only 3% of the anterior gonads have initiated oogenesis at 6 hours after the adult molt (Fig. 1, B and C). Although the devel-

Department of Biology, McGill University, 1205 Avenue Docteur Penfield, Montréal, Québec, Canada, H3A 1B1.

*Present address: RIKEN Center for Developmental Biology, 2-2-3 Minatojima Minamimachi, Chuo-ku, Kobe 650-0047, Japan.
†To whom correspondence may be addressed. E-mail: siegfried.hekimi@mcgill.ca